Water Research 186 (2020) 116410

Contents lists available at ScienceDirect

Water Research

journal homepage: www.elsevier.com/locate/watres

Metal sorption onto nanoscale plastic debris and trojan horse effects in *Daphnia magna:* Role of dissolved organic matter

Fazel Abdolahpur Monikh[a,*], Martina G. Vijver[a], Zhiling Guo[b], Peng Zhang[b], Gopala Krishna Darbha[c], Willie J.G.M. Peijnenburg[a,d]

[a] Institute of Environmental Sciences (CML), Leiden University, P.O. Box 9518, 2300 RA Leiden, Netherlands
[b] School of Geography, Earth and Environmental Sciences, University of Birmingham, Edgbaston, Birmingham, B15 2TT, UK
[c] Department of Earth Sciences & Centre for Climate and Environmental Studies, Indian Institute of Science Education and Research Kolkata, Kolkata, Mohanpur, West Bengal, 741246, India
[d] National Institute of Public Health and the Environment (RIVM), Center for Safety of Substances and Products, Bilthoven, Netherlands

ARTICLE INFO

Article history:
Received 15 July 2020
Revised 24 August 2020
Accepted 7 September 2020
Available online 7 September 2020

Keywords:
Adsorption
Absorption
Particle size
Chemical composition
Silver ions
Oxidative stress

ABSTRACT

There is a debate on whether the Trojan horse principle is occurring for nanoscale plastic debris (NPD < 1 μm). It is realized that NPD have a high capacity to sorb environmental contaminants such as metals from the surrounding environment compared to their microplastic counterparts, which influences the sorbed contaminants' uptake. Herein, we studied the influence of dissolved organic matter (DOM) on the time-resolved sorption of ionic silver (Ag^+) onto polymeric nanomaterials, as models of NPD, as a function of particle size (300 and 600 nm) and chemical composition [polystyrene (PS) and polyethylene (PE)]. Subsequently, the toxicity of NPD and their co-occurring (adsorbed and absorbed) Ag^+ on *Daphnia magna* was determined. Silver nitrate was mixed with 1.2×10^5 NPD particles/mL for 6 days. The extent of Ag^+ sorption onto NPD after 6 days was as follows: 600 nm PS-NPD > 300 nm PS-NPD > 300 nm PE-NPD. The presence of DOM in the system increased the sorption of Ag^+ onto 300 nm PS-NPD and PE-NPD, whereas DOM decreased the sorption onto 600 nm PS-NPD. Exposure to 1 mg/L NPD or 1 μg/L Ag^+ was not toxic to daphnids. However, the mixture of these concentrations of PS-NPD and Ag^+ induced toxicity for both sizes (300 and 600 nm). The addition of DOM (1, 10 and 50 mg/L) to the system inhibited the combined toxicity of Ag^+ and NPD regardless of the size and chemical composition. Taken together, in natural conditions where the concentration of DOM is high e.g. in freshwater ecosystems, the sorption of metals onto NPD depends on the size and chemical composition of the NPD. Nevertheless, under realistic field conditions where the concentration of DOM is high, the uptake of contaminants in D. magna that is influenced by the Trojan horse principles could be negligible.

1. Introduction

The concern with regard to the occurrence of nanoscale plastic debris (NPDs, size < 1 μm) (Sobhani et al., 2020) in the environment is increasing, as they have been assumed to occur in different ecosystems ranging from soils and snow to surface waters and sediments (Alimi et al., 2018; Enfrin et al., 2019; Koelmans et al., 2019; Materić et al., 2020). NPD are mostly formed as a result of plastic weathering, where plastics in the environment break down to small pieces known as microplastics (1 μm < size < 5 mm) (Zhu et al., 2020) and NPD (He et al., 2020). It was reported that NPD can penetrate the biological barriers of organisms and distribute in the organisms' bodies (Al-Sid-Cheikh et al., 2018; Gaspar et al., 2018), which make NPD potentially hazardous to organisms. For example, NPD reduced the body growth, activity and survival of organisms, and induced physiological stress and cell death in exposed organisms (Chae and An 2017; Lee et al., 2019; Liu et al., 2019; Zhu et al., 2020).

Physicochemical properties of plastic particles such as size and chemical composition may induce different toxic responses to the same mass of NPD in organisms (Dong et al., 2018; Jeong et al., 2016). Although the toxicity of NPD to different organisms has been documented (Hanna et al., 2018; Heinlaan et al., 2020), the toxicity of NPD as a function particle size and chemical composition is still largely unknown. For example, Sun et al. (2018) showed a strong correlation between toxicity and size of plastic particles,

* Corresponding author.
E-mail address: f.a.monikh@cml.leidenuniv.nl (F. Abdolahpur Monikh).

https://doi.org/10.1016/j.watres.2020.116410

where NPD induced oxidative stress and rather than microplastics influenced the growth inhibition, chemical composition and ammonia conversion efficiency of *Halomonas alkaliphila* (Sun et al., 2018). A previous study (Lee et al., 2019) showed that small-sized NPD readily penetrated the chorion of developing embryos of zebrafish and accumulated throughout the whole body, mostly in lipid-rich regions. The NPD induced effects on the survival, hatching rate, developmental abnormalities, and cell death of zebrafish embryos as a function of particle size (Lee et al., 2019).

The hazard of NPD may not be limited to the physicochemical properties of the NPD alone, but might also be attributed to the co-occurring chemicals in NPD, such as additives (Toussaint et al., 2019) and/or adsorbed and absorbed chemicals from the surrounding environment onto NPD (Liu et al., 2018; Velzeboer et al., 2014). For example, the so-called "Trojan-horse" principle, a mechanism in which particles serve as vectors to carry chemicals (Naasz et al., 2018; Vale et al., 2014; Xia et al., 2012) into cells and organisms, has been proposed as a relevant pathway for the toxicity of nanomaterials. This toxicity pathway may be extrapolated to NPD as they are also considered as nanoscale materials (Jeong et al., 2018). But the question is whether physicochemical properties of NPD modulate their capability in transferring contaminant into organisms.

Plastics have a high sorptive capacity (absorption and adsorption) for chemicals such as organic compounds and metals (Bakir et al., 2012; Davranche et al., 2019; Ogata et al., 2009). With regard to microplastics, it was documented that plastic particles can act as compartments for the partitioning of chemicals, concentrating chemicals from the surrounding environment (Lee et al., 2014; Tourinho et al., 2019). Recent summaries reported that microplastics are not likely to increase significantly the level of soluble chemicals in organisms upon ingestion (Koelmans et al., 2016; Ziccardi et al., 2016). However, this finding may not necessarily be valid for NPD, which have a much smaller size and a greater volume-specific surface area (VSSA) than their microplastic counterparts (Liu et al., 2018). The sorption capacity of plastic particles increases with decreasing particle size (Wang and Wang 2018; Zhan et al., 2016) and increasing VSSA and the time needed to reach partition equilibrium may significantly differ compared to microplastics counterparts.

When NPD enter the environment they immediately interact with natural organic matter (NOM) resulting in the formation of NOM-coated NPD. NOM originate from the degradation of plants and animals residuals in the environment and is ubiquitous at different concentrations in natural surface water (Murphy et al., 1999). The presence of NOM on the surface of NPD not only influences the colloidal stability of the particles (Shams et al., 2020) but might also influence the sorption of chemicals onto the NPD. As a result, the amount of chemicals sorbed to the NPD might change as a function of NOM concentration (Wu et al., 2016; Yu et al., 2019). Decreased (Wu et al., 2016) and increased sorption (Chen et al., 2017) of chemicals in the presence of NOM has been already reported. This can, consequently, alter the toxicity profile of the NPD and their co-occurring contaminants. Although the influence of NOM on the toxicity profile of microplastics was investigated (Qiao et al., 2019), there is no study available to show how the presence of NOM may influence the sorption of chemicals onto NPD and eventually the Trojan horse effect of NPD in aquatic organisms. Other environmental parameters such as salinity and pH may also influence the sorption of chemicals onto NPD (Alimi et al., 2018). This necessitates understanding the sorption of chemicals to NPD and their subsequent toxicity to organisms under environmentally relevant conditions rather than in pure water. NOM contains many reactive groups, such as hydroxyls, amines, thiols, and carboxylic acids that can complex with chemicals and alter, mostly decrease, the bioavailability and, subsequently, the toxicity of the chemicals (Kungolos et al., 2006; Roy and Campbell 1997; Wang et al., 2016). In case of metal, for example, NOM can influence the speciation of metals and alter their toxicity (Kungolos et al., 2006). It is important to understand whether this can be extrapolated to a system in which NPD are present.

In this study, we investigated the sorption of silver (Ag^+) ions onto 300 and 600 nm polystyrene (PS) nanomaterials and 300 nm polyethylene (PE) nanomaterilas as models of NPD in the presence and absence of dissolved organic matter (DOM) for 6 days. The sorption experiments were performed in a standard exposure medium of *Daphnia magna* (Elendt M7 medium pH 8) to mimic natural condition as much as possible. It is well documented that Ag^+ is a toxic and non-essential metal to organisms, which can cause oxidative stress in organisms (Bury et al., 1999b; Hogstrand et al., 1996). We investigated how NPD influence the toxicity profile of Ag^+in the presence and absence of DOM.

2. Materials and methods

2.1. Materials

All chemicals used to prepare the culture media for *D. magna*, to prepare samples for chemical analysis, and to determine the biochemical biomarkers were of analytical grade and purchased from Sigma-Aldrich (Zwijndrecht, the Netherlands) or Merck (Darmstadt, Germany). Spherical PS nanomaterials with an average size of 600 nm (PDI = 0.08) and 300 nm (PDI = 0.02) were purchased from Microparticles GmbH Forschungs (Berlin, Germany) and Thermo Fisher Scientific (Bleiswijk, the Netherlands), respectively, to be used as a model of PS-NPD in this study. The PS-NPD were supplied in a liquid dispersion. Spherical PE-materials of 300–9000 nm were purchased from Cospheric LLC (Santa Barbara, CA, US) to be used as a model of PE-NPD. The PE-NPD was supplied as a powder. Silver nitrate ($AgNO_3$), nitric acid (HNO_3, 65%) and sodium hydroxide (NaOH) were purchased from Sigma-Aldrich (Sigma-Aldrich Corp., St. Louis, MO, USA). Ag^+ standards with concentrations of 1000 mg/L were obtained from PerkinElmer (Rotterdam, the Netherlands). Suwannee River NOM (1R101N) was purchased from the International Humic Substances Society (Saint Paul, Minnesota, United States).

2.2. Characterization of NPD in different media

The PS-NPD of different sizes (600 and 300 nm) were dispersed in Millì-Q (MQ) water (10 mg/L) and sonicated using a bath sonicator (35 kHz frequency, DT 255, Bandelin electronic, Sonorex digital, Berlin, Germany) for 5 min and used as stocks for the PS-NPD. The PE-NPD were dispersed in ethanol (30%) and sonicated using a bath sonicator for 5 min. After sonication, the dispersion of PE-NPD was filtered through a Whatman filter paper of 400 nm cut-off and the filtrate was used as a stock of PE-NPD. The particle number concentration of the NPD in the stock dispersions was measured using Nanoparticle Tracking Analyzer (NTA, NanoSight's NS200, Malvern, the Netherlands) and kept at around 30×10^6 particles/mL. It is reported that NTA produces a number-based distribution and can deal with polydisperse samples (Abdolahpur Monikh et al. 2019a). We therefore used this technique to measure the NPD particle number.

For imaging the NPD, aliquots of the dispersion were diluted (with MQ for PS-NPD and with 0.01% ethanol for PE-NPD), put on copper grids and left to dry out for 24 h. A JEOL 1400 transmission electron microscope (TEM) operating at 80 kV accelerating voltage was used to image the NPD and determine their shape and size distribution. A Zetasizer Nanodevice (Malvern Panalytical, Netherlands) was used to determine the hydrodynamic size and

zeta potential of the NPD in the samples. Accordingly, aliquots of the dispersion were diluted with MQ water and immediately measured with regard to zeta potential and hydrodynamic size. It is possible that the NPD undergo aggregation in the exposure media. To determine the aggregation profile of the NPD in the exposure media, the hydrodynamic size of the particles in the exposure medium was measured over time according to our previous study (Abdolahpur Monikh et al. 2019c).

2.3. Sorption experiments

The sorption experiments to NPD were carried out using a batch adsorption approach (Liu et al., 2018) in the presence and absence of DOM in the exposure medium (Elendt M7 medium pH 8) which was used to culture *D. magna*. The experimental design and the treatments are illustrated in Fig. 1a. Ten replicates were used for each treatment. The NPD were dispersed in the exposure medium to reach a final nominal concentration of 1.2×10^5 particles/mL and sonicated for 5 min. We must emphasize that the particle number concentration might be dynamic and the particle number concentration refers to the initial concentration. $AgNO_3$ (46.9% as Ag^+) was added to the dispersion to reach a final concentration of 100 μg/L Ag^+.

We used a high concentration of Ag^+ because we assumed that a part of the Ag^+ added would bind to Cl^- to form insoluble AgCl. To obtain the DOM suspensions, NOM was dissolved in MQ water following the method reported by Arenas Logo et al. (Arenas-Lago et al., 2019) and filtered through a Whatman filter paper of a 0.45 μm cut-off. The final concentration of the DOM in the filtrate was ~ 450 mg/L. DOM was added to the mixture of NPD and Ag^+ to reach a final concentration of 1, 10 or 50 mg/L of DOM (Fig. 1a). All samples were covered with parafilm and shaken on a rotator (at 18 rpm) in the dark at 4 °C for 6 days. Aliquots of the samples were taken every day for 6 days in total and centrifuged (Thermo Scientific Sorvall ST 16R Centrifuge) at 3000 × *g* for 20 min. To assure that the centrifugation force has removed the NPD from the supernatant (top 2 mm), in a separate sample the NPD were dispersed in MQ water and centrifuged at 3000 × *g* for 20 min. After centrifugation, the particle number in the 2 mm supernatant was measured using NTA. No particles could be detected in the supernatant after centrifugation, which confirms the removal of the NPD from the top 2 mm of the supernatant. Control samples including Ag^+, DOM, and a mixture of Ag^+ and DOM without NPD were also used alongside the samples. The Ag^+ control without NPD was used to evaluate the formation of insoluble Ag^+ in the samples which may lead to the removal of Ag^+ from the supernatant after centrifugation. The supernatants were removed and digested using *aqua regia* (3 ml HCl: 1 ml HNO_3) for 1 h at 70 °C in a water bath. The residuals were diluted to a final volume of 15 mL and the Ag^+ concentration in the samples was measured using inductively coupled plasma mass spectrometry (ICP-MS).

2.4. Immobilization assay with D. magna

For the acute immobilization tests with *D. magna*, the neonates less than 24 h old were separated and cultured for the experiments. When they became adult (after 9 days), the adult *D. magna* were cultured in a 200 mL of Elendt M7 medium with an average of three organisms per beaker. The young adults were tested because at this stage they are large enough to have particles sized 600 nm as food items. Acute immobilization was determined following the methods described within OECD guidelines (202) (OECD 2004). Five replicates per treatment were tested (15 organisms per each treatment). The organisms were kept at 22 °C with a 16 h light: 8 h dark cycle. The daphnids were fed 3 times per week prior to the exposure with 100 mg of wet weight green microalgae per daphnia.

The *D. magna* were exposed to NPD and different concentrations of Ag^+ and DOM as illustrated in Fig. 1b for each size and type of NPD, separately. The exposure was performed with mixtures of all possible combinations of NPD (initial concentration of 6.74×10^{10} particles/L), Ag^+ (0, 1, 2, 5 and 10 μg/L) and DOM (0, 1, 10 and 50 mg/L) (Fig. 1b). These DOM concentrations were selected to represent a range that occurs in various natural surface waters (Chaves et al., 2011). Ag^+ concentrations were selected based on previous studies (Bianchini and Wood 2003; Shen et al., 2015). A detailed explanation of the exposure conditions is provided in the S1, Supporting Information. The organisms were exposed to a mixture of the Ag-DOM-NPD after the Ag^+ concentration in the supernatant almost reached a steady-state. After 72 h of exposure, the number of immobile daphnids in each treatment was counted to obtain the percentage of survival per treatment.

2.5. Sublethal toxicity measurements

The sublethal effects of Ag^+ were determined by measuring the bioconcentration factor (BCF) of Ag^+, to determine the uptake of Ag^+ in the organisms and prove the Trojan horse principle. The activity of superoxide dismutase (SOD), catalase (CAT), and glutathione peroxidase (GPx) were determined to monitor the oxidative stress induced by Ag^+. The sublethal toxicity was only determined within organisms that did not die and measurements were restricted to the 1 μg/L Ag^+ treatment.

2.5.1. Determining the BCF of Ag

After exposure for 72 h, 1 ml of the exposure media was taken and analyzed to determine the concentration of Ag^+ in the exposure media. The organisms were removed and put in clean media for 24 h as a depuration period. Depuration experiments were performed to allow the organisms to empty their gut. Our hypothesis is that the fraction of the NPD that could not pass the gut epithelium and internalize into the organisms is excreted during the depuration period. The 24 h depuration time was arbitrary selected according to previous studies which showed that after 24 h depuration considerable amounts of NPD are removed from the gut of *D. magna* (Rist et al., 2017). After 24 h, the organisms were removed, cleaned gently with tap water and dried at 60 °C to constant weight. The dried organisms were weighted and digested using *aqua regia* for 1 h at 70 °C in a water bath. The residuals were diluted and the Ag^+ concentration in the samples was measured to obtain the BCF of Ag^+ for each treatment separately. The BCF of Ag^+ was calculated as follows in which the possible adsorption on organisms and absorption in organisms were taken as the total mass concentration in the organisms (after 24 h of depuration):

$$BCF\ (L/Kg) = \frac{Totall\ mass\ concenetration\ of\ Ag\ in\ and\ on\ organisms\ (\mu g/Kg)\ at\ 72\ h}{Totall\ mass\ concnentration\ of\ Ag\ in\ exposure\ media\ (\mu g/L)\ at\ 72\ h}$$

2.5.2. Determination of biochemical biomarkers

The activities of SOD, CAT and GPx were measured following previously reported methods as described below. Briefly, the organisms were homogenized using a glass homogenizer in 10 vol (w:v) ice-cold 10 mM potassium phosphate buffer (pH 7.4) for 2 minutes at 3000 rpm. The homogenates were then centrifuged at 10,000 × *g* for 20 min at 4 °C, and the supernatant was removed and kept at −80 °C for enzymatic assay. The SOD activity was determined at 420 nm by determining the rate of pyrogallol autooxidation for 3 min using Ultraviolet-visible spectroscopy (UV–vis) following the method reported previously (MARKLUND and MARKLUND 1974). The CAT activity, as measured by hydrogen peroxide consumption, was assayed at 240 nm using UV–vis following the method reported by Aebi (Bergmeyer 1974). GPx activity, estimated

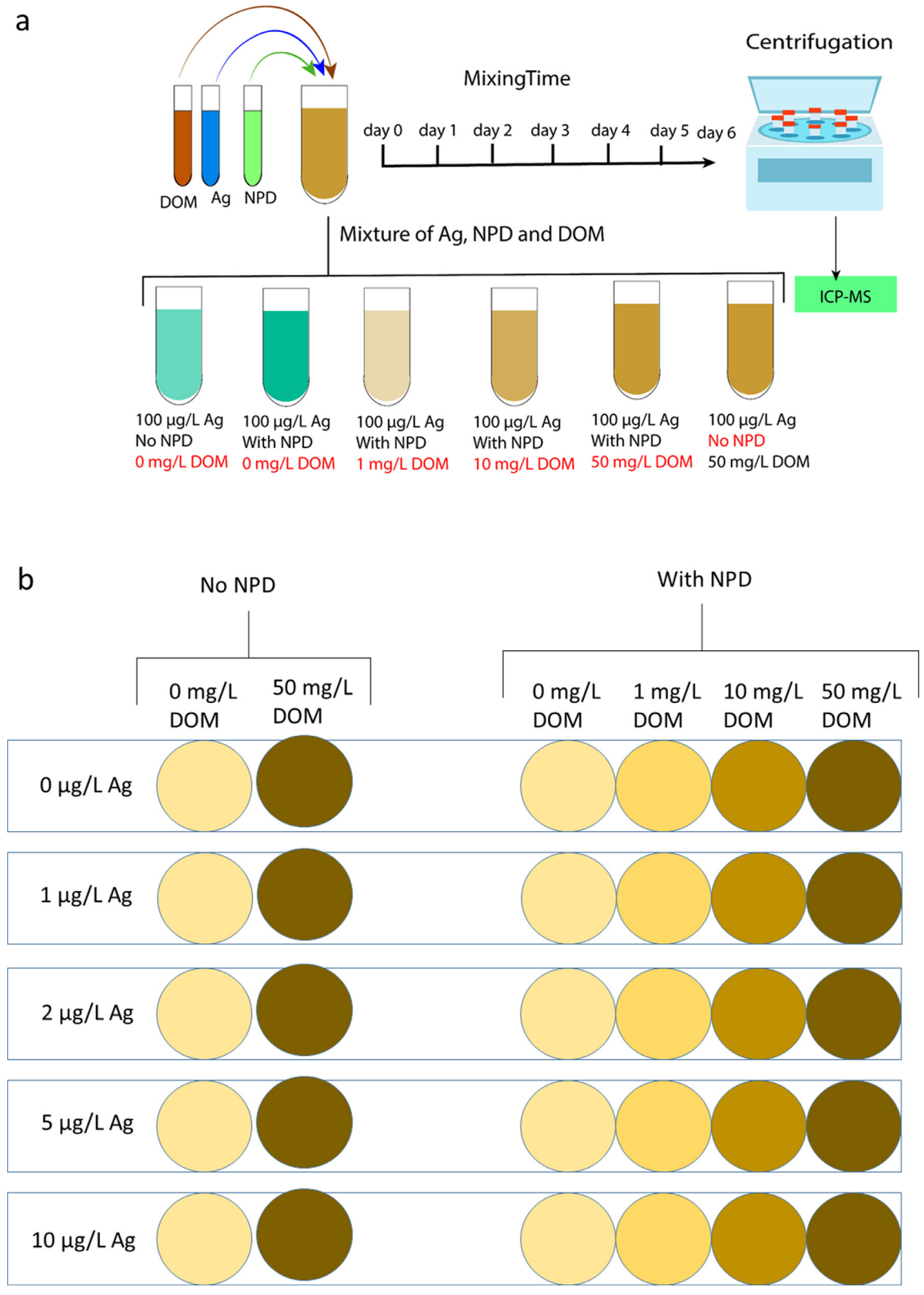

Fig. 1. Schematic illustration of the experimental design. a) The sorption experiment for (silver) Ag+ onto nanoscale plastic debris (NPD) in the presence and absence of dissolved organic matter (DOM). b) Treatments used for exposure of D. magna to different combinations of Ag+, NPD and DOM.

by the rate of nicotinamide adenine dinucleotide phosphate oxidation, was assayed at 340 nm using UV–vis according to the method reported by Drotar et al. (Drotar et al., 1985). Controls without enzymes were subtracted from the total rate to yield the enzymatic activity rate. The activities of the enzyme were reported after normalization with the value obtained for the control.

2.6. Ag measurements in the samples

The Ag^+ concentration in water samples and the Ag^+ body burden in the organisms were measured using ICP-MS. A PerkinElmer NexION 2000 ICP-MS operating in standard mode was used for this purpose. The conditional set up of the ICP-MS is given in Table S1 (Supporting Information).

2.7. Data analyses

The IBM SPSS Statistics 25 software was used to run the statistical analyses of the data. The normality and homogeneity of variances were checked using Kolmogorov-Smirnov and Levene tests, respectively. The results are expressed as the mean ± standard deviation (SD). One-way ANOVA followed by Dunnett's test was used to evaluate the significant differences between Ag^+ sorption onto NPD of different types, in the presence of various concentrations of DOM, and to evaluate the toxicity of Ag+ to daphnids exposed to different treatments. The difference between the sorption of Ag^+ onto 300 nm PS-NPD and 300 nm PE-NPD and also the difference between PS-NPD of different particle sizes were measured using a *t-test*. Differences were considered to be significant at $P < 0.05$.

3. Results and discussion

3.1. NPD characterization

The obtained TEM images for the NPD (Figure S1, Supporting Information) indicated that the particles were spherical in shape with a narrow size distribution. The sonication force did not break the particles. In MQ water, the hydrodynamic size of the particles was around 730 ± 45 nm, 320 ± 28 nm and 410 ± 85 nm and the zeta potential was -38 ± 3 mV, -34 ± 2 mV and -43 ± 3 mV for 630 nm PS-NPD, 300 nm PS-NPD and 300 nm PE-NPD, respectively. This high absolute value of the zeta potential is indicative of the electrostatic stability of the particles against agglomeration. The physicochemical properties of the NPD in 50 mg/L DOM solution is reported in Table S2 (Supporting Information). When the particles were dispersed in the exposure media the absolute value of the zeta potential decreased to -24 ± 4, -21 ± 3 and -32 ± 4 for 630 nm PS-NPD, 300 nm PS-NPD and 300 nm PE-NPD, respectively. This could lead to particle agglomeration over time for, particularly, the 300 nm and 600 nm PS-NPD. We indeed determined a slight increase in the hydrodynamic size of the PS-NPD over 48 h measurement (Fig. 2a). However, the hydrodynamic size of the PE-NPD increased dramatically over 48 h. We obtained the PS-NPD in liquid, meaning that the surface of PS-NPD was modified to make the particles dispersible in aqueous media. On the other hand, the PE-NPD was powder and we dispersed them in water using ethanol. Thus the obtained fast aggregation for PE-NPD is highly likely to be attributed to the hydrophobic force that attracts the PE-NPD together and not because of the electrostatic force as the particle had a highly negative zeta potential in the exposure media.

3.2. Sorption of silver onto NPD in the presence and absence of DOM

In this study, we did not focus on the influence of the electrolyte on the Ag^+ sorption onto the NPD and we restricted the study to determine the final influence of the exposure medium (as an environmentally relevant medium) on the NPD and their capacity in adsorbing and absorbing Ag^+. Our results confirm that the size and chemical composition of the NPD can influence the sorption of Ag^+ onto NPD. Fig. 2b-d shows the time-resolved sorption of Ag^+ onto the NPD in the presence and absence of DOM. In the treatment without NPD and DOM, the concentration of Ag^+ in the supernatant remained relatively stable over 6 days of mixing (Fig. 2b), suggesting that the formation of insoluble Ag^+ could be neglectable or the insoluble Ag^+ did not sediment over time. The presence of DOM also did not influence the quantity of Ag^+ in the supernatant (Fig. 2b). This is in agreement with our previous studies for DOM and copper (Cu), where the presence of DOM did not decrease the quantity of Cu in the supernatant after centrifugation (Arenas-Lago et al., 2019).

In the treatment containing 300 nm PS-NPD (Fig. 2b), the concentration of Ag^+ decreased in the supernatant over time, indicating that Ag^+ is ab/adsorbed onto the surface of the particles and was removed from the supernatant after centrifugation. This finding is in agreement with a previous study which showed that metals such as Ag^+ are ad/absorbed onto PS particles (Kalčíková et al., 2020). Note that there might be desorption of Ag^+ from the NPD back into the medium. However, we could not observe this because it might occur within the few primary hours of the exposure (Liu et al., 2018). The sorption of Ag^+ onto the 300 nm NPD reaches a steady-state after 1 day. DOM increased the sorption of Ag^+ onto the particles as confirmed by the reduced amount of Ag^+ in the supernatant. Increasing the concentration of the DOM from 1 mg/L to 50 mg/L significantly (ANOVA, $p < 0.05$) decreased the quantity of Ag^+ in the supernatant. This indicates that the sorption of Ag^+ onto the NPD increased. DOM has a variety of functional groups such as carbonyl, carboxyl, aromatic, acetal, and phenolic groups which allows for complexation with metal ions (Iskrenova-Tchoukova et al., 2010; Karlsson et al., 2005). When the Ag^+ absorbs to the DOM that is attached to the surface of the NPD, the quantity of Ag^+ in the supernatant decreases after centrifugation as a result of NPD sedimentation. This is in agreement with the literature, as it is reported that NOM attached to the surface of nanomaterials e.g. Fe_3O_4 (Liu et al., 2008), TiO_2 (Chen et al., 2012) and carbon nanotubes (Tian et al., 2012) increases the removal of metals from water. This can explain the higher removal of Ag^+ from the supernatant by DOM-coated NPD compared to the bare NPD.

Our finding showed that the sorption of Ag^+ onto PS-NPD is a function of PS-NPD size, as the 300 nm PS-NPD ad/absorbed a lower amount of Ag^+ compared to the 600 nm PS-NPD (Fig. 2c). In this experiment, we kept the particle number concentration equal for all the treatments. The comparison between NPD is on a particle number concentration basis and not on a mass basis. Therefore the available surface for sorption of Ag^+ in the treatment with 600 nm particles (1.36×10^{-3} cm^2) is larger than in the treatment with 300 nm (3.4×10^{-4} cm^2), which could explain the higher quantity of Ag^+ removed from the supernatant by the 600 nm PS-NPD. The sorption of Ag^+ onto the 600 nm PS-NPD reached a steady-state roughly after 3 days of incubation. Sorption of chemicals onto NPD involves absorption in and adsorption on the NPDs (Alimi et al., 2018; Rochman et al., 2013a). The 600 nm PS-NPD have a larger volume compared to the 300 nm PS-NPD. Although surface adsorption of chemicals may reach a steady-state a few hours after the exposure (Liu et al., 2018), the diffusion of Ag^+ into the NPD matrix and absorption into the particle with a larger volume may take a longer time. Interestingly, the presence of DOM decreased the sorption of Ag^+ onto the 600 nm PS-NPD compared to the 300 nm PS-NPD. It is likely that the attached DOM on the surface of the NPD acts as an absorbent layer which absorbs Ag^+ ions. When the DOM layer reaches saturation, further diffusion of Ag^+ into the NPD is electrostatically unfavorable. This can be con-

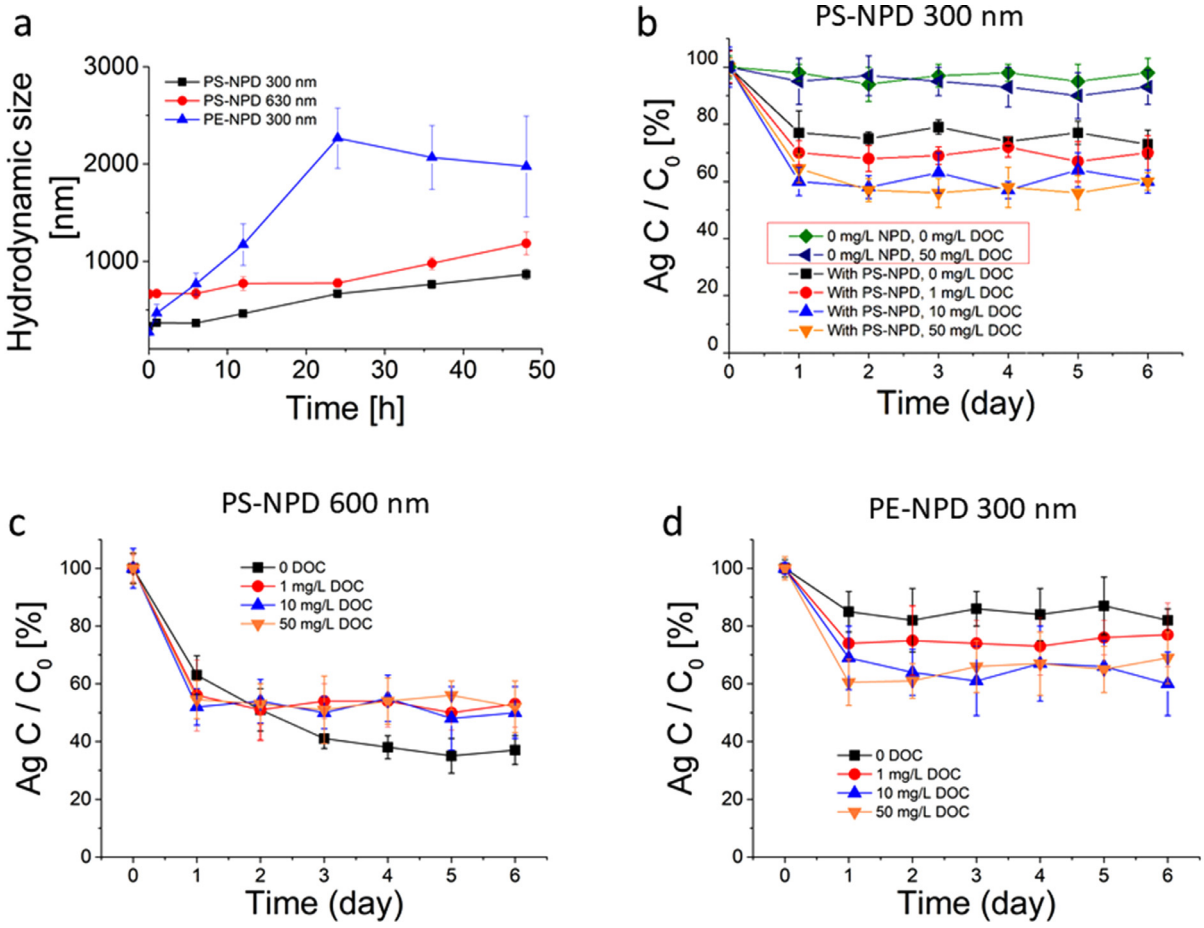

Fig. 2. a) The agglomeration of the NPD in the exposure medium over time. b-d) It shows the removal of Ag+ ions from the supernatant of the treatments contain 300 nm PS-NPD (b), 600 nm PS-NPD (c) or 300 nm PE-NPD (d) and different concentration of DOM over 6 days of mixing.

firmed by reaching an earlier steady-state in the presence of DOM compared to the naked NPD (Fig. 2c).

We also demonstrated that the chemical composition of NPD plays a significant role in the sorption of Ag^+ onto the particles. In the treatment containing PE-NPD and Ag^+ (Figure 3d), the concentration of the removed Ag^+ from the supernatant after centrifugation decreased over time, suggesting the sorption of the Ag^+ onto the PE-NPD. However, the quantity of the ab/adsorbed Ag^+ onto the 300 nm PE-NPD was significantly (*t-test*, $p < 0.05$) lower than the ab/adsorbed Ag^+ onto the 300 PS-NPD. The two NPD were similar in size (300 nm) and shape (spherical) but varied in polymeric chemical composition. The PE-NPD has a relatively rubbery and flexible structure at room temperature and is expected to allow for greater diffusion of the chemical into the matrix of the NPD as compared to PS-NPD (Liu et al., 2018; Pascall et al., 2005), as the PS-NPD has a dense, glassy polymeric structure (Liu et al., 2018) which limits the absorption of chemicals. However, this generalization did not hold in our findings. A possible explanation for this is the fast agglomeration of the PE-NPD (Fig. 2a), which can decrease the available surface area for sorption of Ag^+ onto the particles. The presence of DOM increased the total quantity of Ag^+ removed from the medium by the PE-NPD, confirming our hypothesis that aggregation decreases the capacity of chemical sorption by PE-NPD. DOM increased the stability of the PE-NPD due to steric stabilization as observed for other NPD (Oriekhova and Stoll 2018). This consequently increases the available surface area for chemical sorption as previously observed for DOM-coated carbon nanotubes (Tian et al., 2012). Increasing the concentration of the DOM from 1 mg/L to 50 mg/L, increased the removal of Ag^+ from the supernatant by PE-NPD.

3.3. *The toxicity of Ag-DOM-NPD cocktails to* D. magna

3.3.1. *Immobilization bioassay*

The results of the immobilization bioassays are reported in Table 1. The PS-NPD and the PE-NPD did not induce any mortality to the organism when compared to the control (without any chemical). It is well known that Ag^+ could be a toxic metal to organisms including *D. magna* even at trace levels of 1–10 μg/L (Glover et al., 2005). In this study, the immobilization bioassay showed that 1 μg/L Ag^+ did not induce lethal toxicity to *D. magna* (Table 1). However, in the presence of PS-NPD of 300 nm and 600 nm, the concentration of 1 μg/L Ag^+ led to mortality to the organisms, where the survival decreased to 64% ± 2.5 and 85% ± 1 in comparison to the control (without any chemicals), respectively. The PE-NPD did not change the toxicity profile of 1 μg/L Ag^+ compared to the PS-NPD and the control. It is clear that the presence of PS-NPD led to an increased toxicity of Ag^+. It is possible that PS-NPD increase the bioavailability and uptake of the Ag^+in the daphnids or change the uptake pathway of the Ag^+. The PS-NPD may for example facilitate the transport of Ag^+ ions into an organ within the daphnids whilst the Ag^+ ions alone cannot target that organ. When the Ag^+ concentration in the exposure media increased (from 0 to 10 μg/L) the survival of *D. magna* decreased (from roughly 98% to 0). The toxicity in the presence of 300 nm PS-NPD was higher than in the presence of 600 nm PS-NPD and 300 nm PE-NPD. Although a previous study showed that NPD may

Table 1
Survival of D. magna exposed to NPD (6.74 × 1010 particles/L) and various concentrations of Ag ions and dissolved organic matter (DOM) for 72 h.

Ag (μg/L)	Control (without NPD and DOM)	Control with 50 mg/L DOM (without NPD)	NPD (1 mg/L)	Control with NPD (without DOM)	Cocktail of NPD and 1 mg/L DOM	Cocktail of NPD and 10 mg/L DOM	Cocktail of NPD and 50 mg/L DOM
0	97% ± 0.3	98% ± 0.6	300 nm PS-NPD	97% ± 1.2	96% ± 1	98% ± 0.2	96% ± 0.5
			600 nm PS-NPD	98% ± 0.6	97% ± 0.3	94% ± 0.6	97% ± 0.7
			300 nm PE-NPD	95% ± 0.5	96% ± 0.3	97% ± 0.6	95% ± 0.4
1	98% ± 0.2[b]	97% ± 0.5[b]	300 nm PS-NPD	64% ± 2.5[a]	96% ± 0.8 [b]	95% ± 0.6 [b]	97% ± 0.4 [b]
			600 nm PS-NPD	85% ± 1[a]	98% ± 0.3 [b]	94% ± 0.7 [b]	98% ± 0.5 [b]
			300 nm PE-NPD	95% ± 1.5[b]	96% ± 0.5 [b]	97% ± 0.4 [b]	95% ± 0.8 [b]
2	61% ± 11[b]	96% ± 0.7[c]	300 nm PS-NPD	47% ± 13[a]	94% ± 1 [c]	97% ± 0.4 [c]	96% ± 0.7 [c]
			600 nm PS-NPD	69% ± 7[b]	95% ± 1.5 [c]	93% ± 0.9 [c]	94% ± 0.4 [c]
			300 nm PE-NPD	63% ± 10 [b]	96% ± 0.8 [c]	96% ± 0.6 [c]	95% ± 0.8 [c]
5	0[a]	56% ± 14[c]	300 nm PS-NPD	0[a]	34% ± 17 [b]	52% ± 10 [c]	71% ± 13 [d]
			600 nm PS-NPD	0[a]	74% ± 12 [d]	82% ± 7 [d]	80% ± 6 [d]
			300 nm PE-NPD	0[a]	38% ± 15 [b]	47% ± 13 [c]	74% ± 11 [d]
10	0	0	300 nm PS-NPD	0	0	0	13% ± 5
			600 nm PS-NPD	0	0	0	10% ± 4
			300 nm PE-NPD	0	0	0	15% ± 3

a–d indicate significant differences between the treatments ($P<0.05$). Data are presented as means ± standard deviation (SD) of 15 organisms.

increase the toxicity of metals due to the Trojan horse mechanism (Lee et al., 2019), our study for the first time shows that the size and chemical composition of NPD influence the toxicity of Ag^+ to *D. magna*. Overall, our findings not only showed that due to the Trojan horse mechanism, the NPD increased the lethal toxicity of the Ag^+, but also confirmed that the smaller NPD are more hazardous compared to the larger particles of the same chemical composition.

The presence of DOM at concentrations of 1 mg/L up to 50 mg/L reduced the combined toxicity of Ag-NPD for all the tested NPD regardless of size and chemical composition. This is in agreement with a previous study which showed that NOM decreases the toxicity of PS-NPD to *D. magna* (Fadare et al., 2019). DOM binds Ag^+ ions and prevents the ions from binding to the site of toxic action (Glover et al., 2005). In the presence of 5 μg/L Ag^+, the DOM could not totally inhibit Ag^+ toxicity and the DOM-coated 300 nm PS-NPS induce higher toxicity compared to the DOM-coated 600 nm PS-NPD. The toxicity of Ag^+ in the presence of the DOM-coated NPD was not affected by the chemical composition of the NPD, because there was no difference between the toxicity induced by DOM-coated PS-NPD and DOM-coated PE-NPD of the same size. It is likely that DOM offers a similar surface composition to NPD regardless of the chemical bulk composition of the particles, which in return determines the interaction of the NPD with organisms. Apparently, DOM decreases the toxicity of metals in aquatic organisms independent of the metals being present in their dissolved form or sorbed onto NPD by decreasing their bioavailability to the organisms.

3.3.2. Bioconcentration of Ag

Organisms exposed to 1 μg/L Ag^+ showed the highest survival rate compared to other treatments. Thus, we selected 1 μg/L Ag^+ concentration to investigate the sublethal toxicity in *D. magna*. First, we must understand whether Ag^+ is taken up and bioconcentrate in the organisms from the exposure media and how the presence of NPD and DOM influences the Ag^+ uptake. The BCFs of Ag^+ were calculated in organisms exposed to 1 μg/L Ag^+, 6.74×10^{10} particles/L NPD, and different concentrations of DOM. The results (Table 2) showed that the BCFs of Ag^+ in the organisms exposed to the mixture of NPD and Ag^+ were significantly higher than the BCFs of the other treatments and higher than the BCF for the organisms exposed to Ag^+ alone. This is in agreement with a previous study investigating the mixture effects of Ni and microplastics in *D. magna*, where the exposure to the mixture of the microplastics and Ni led to a higher BCF of Ni compared to the exposure to Ni alone (Kim et al., 2017). This supports our hypothesis that NPD increase the uptake of Ag^+ in daphnids. The higher BCF observed for 300 nm PS-NPD (0.7) compared to the 600 nm PS-NPD (0.3) confirms that smaller NPD may increase the uptake of chemicals due to penetration of biological barriers and entering organisms in a higher quantity compared to their larger counterparts. Although the increase in the uptake of chemicals in the presence of microplastics has been documented (Kim et al., 2017; Rochman et al., 2013b), very few studies reported this phenomenon for NPD (Chen et al., 2017; Lee et al., 2019; Ma et al., 2016). For example, Ma et al. (Ma et al., 2016) reported that the presence of 50 nm NPD significantly increased the bioaccumulation of chemicals in *D. magna* and increased the BCF over the entire exposure period. They suggested that unlike microplastics, NPD can easily accumulate on the thoracopods and in the digestive tract (Ma et al., 2016). The BCF of the Ag^+ in the presence of 300 nm PE-NPD was similar to the BCFs calculated for 300 nm PS-NPD. This finding showed that 300 nm PE-NPD and PS-NPD have a similar influence on the uptake of Ag^+regardless of the difference in the chemical composition of the NPD. The NPD of different chemical composition, however, had a different influence on the toxicity profile of Ag^+. As described by Ma et al. (Ma et al., 2016), one explanation could be that the Ag-PE-NPD complexes accumulate on the appendages of the organisms (Ma et al., 2016) due to the hydrophobic surface, which explains the high BCF while no lethal toxicity is observed. Whilst this accumulation did not occur in the case of 300 nm PS-NPD because the surface was modified. The presence of DOM significantly decreases the BCF of Ag^+ in all treatments regardless of NPD size and shapes. The high affinity of DOM for Ag^+ was reported to be responsible for the observed protective effects regarding freshwater organisms in toxicity tests (Bury et al., 1999a; Glover et al., 2005).

3.3.3. Activities of antioxidant enzymes

After confirming that NPD can increase the uptake of Ag^+ in *D. magna* as a function of NPD size and chemical composition, we aimed to understand whether the NPD can also influence the sublethal toxicity of Ag^+ in the organisms. It is well documented that exposure to Ag^+ induces the production of Reactive Oxygen Species (ROS) and, consequently, oxidative stress in organisms (Gomes et al., 2015). Like other organisms, *D. magna* has also developed antioxidant defense mechanisms to balance the naturally formed ROS (Kim et al., 2018; Poynton et al., 2007). Accordingly, *D. magna* uses enzymes such as SOD, CAT, and GPx which are directly involved in the removal of ROS to eliminate the oxidative stress in-

Table 2
The calculated BCF (L/Kg) of Ag+ and antioxidant enzyme activities (SOD, CTA and GPx) in D. magna exposed to 1 μg/L of Ag+, 6.74 × 1010 particles/L of NPD and various concentrations of DOM after 72 h exposure followed by 24 h of depuration. The values obtained for the activity of the SOD, CTA and GPx are normalized by the value obtained for control contains no additives (Ag+, DOM and NPD).

Sublethal end points	Control without any additives	Control with Ag (without NPD and DOM)	Control with 50 mg/L DOM (without Ag and NPD)	Control with NPD (without Ag and DOM)	Control with NPD and DOM (without Ag)	Control with Ag and DOM (without NPD)	NPD (1 mg/L)	Control with NPD and Ag (without DOM)	Cocktail of NPD, Ag and 1 mg/L DOM	Cocktail of NPD, Ag and 10 mg/L DOM	Cocktail of NPD, Ag and 50 mg/L DOM
BCF (L/Kg)		0.1 ± 0.02 [b]				0.05 ± 0.01 [a]	300 nm PS-NPD	0.7 ± 0.1 [c]	0.03 ± 0.01 [a]	0.06 ± 0.01 [a]	0.03 ± 0.01 [a]
							600 nm PS-NPD	0.3 ± 0.06 [c]	0.05 ± 0.01 [a]	0.06 ± 0.02 [a]	0.08 ± 0.01 [a]
							300 nm PE-NPD	0.6 ± 0.3 [c]	0.04 ± 0.01 [a]	0.05 ± 0.02 [a]	0.04 ± 0.01 [a]
SOD	100% [a]	110% ± 3 [b]	95% ± 0.5 [a]	95% ± 0.7 [a]	97% ± 0.4 [a]	103% ± 0.6 [a]	300 nm PS-NPD	125% ± 2.5 [c]	104% ± 1 [a]	97% ± 0.8 [a]	96% ± 0.8 [c]
							600 nm PS-NPD	122% ± 2 [c]	105% ± 1.5 [a]	103% ± 0.6[a]	98% ± 0.6 [a]
							300 nm PE-NPD	127% ± 1.5 [c]	98% ± 0.7 [a]	106% ± 0.5 [a]	105% ± 0.8 [a]
CTA	100% [a]	133% ± 2.5 [b]	97% ± 0.8 [a]	102% ± 0.6 [a]	96% ± 0.5 [a]	98% ± 0.7 [a]	300 nm PS-NPD	146% ± 3 [c]	104% ± 1 [a]	102% ± 0.7 [a]	95% ± 1.5 [a]
							600 nm PS-NPD	137% ± 2 [b]	102% ± 0.6 [a]	95% ± 1 [a]	107% ± 1 [a]
							300 nm PE-NPD	152% ± 2.5 [c]	98% ± 0.5 [a]	107% ± 1.5 [a]	94% ± 1.5 [a]
GPx	100% [a]	128% ± 5 [b]	96% ± 1.5 [a]	104% ± 0.8 [a]	103% ± 0.3 [a]	104% ± 1 [a]	300 nm PS-NPD	141% ± 4 [c]	106% ± 1.5 [a]	95% ± 1 [a]	95% ± 0.8 [a]
							600 nm PS-NPD	133% ± 2 [b]	97% ± 0.5 [a]	103% ± 0.6 [a]	106% ± 0.9 [a]
							300 nm PE-NPD	145% ± 3 [c]	103% ± 0.8 [a]	107% ± 1 [a]	98% ± 0.5 [a]

a–d indicate significant differences between the treatments ($P<0.05$). Data are presented as means ± standard deviation (SD) of 15 organisms.

duced by Ag^+. We measured the activities of these enzymes to determine the oxidative stress induced as a result of exposure to Ag^+. The results (Table 2) showed that the highest biomarker response was observed in *D. magna* exposed to Ag^+ and to the mixture of Ag^+ and NPDs. The increase in the activities of SOD, CAT and GPx indicated that the organisms are responding to the increased levels of ROS. The activities of all analyzed enzymes increased significantly after exposure to the mixture of NPD and Ag^+ compared to Ag^+ alone. This is an indication that NPD enhance the oxidative stress of Ag^+ and the activity of the enzymes increased to eliminate the ROS.

Our findings showed that the activity of SOD was independent of NPD size and chemical composition. However, the activity of CAT and GPx in organisms exposed to 300 PS-NPD was significantly higher than in the organisms exposed to 600 nm PS-NPD. This further confirms that the size of NPD dramatically influences their Trojan horse mechanism, likely due to the higher uptake of the 300 nm particles compared to the 600 nm particles. The organisms exposed to PE-NPD showed higher activities in the CAT and GPx enzymes compared to organisms exposed to 300 nm PS-NPD. Our study for the first time documents that the chemical composition of NPD influences their Trojan horse effect. Interestingly, in the presence of DOM, the activity of the enzymes was not significantly different from to the activity measured in control organisms. Previous studies reported that DOM sorbed to particles inhibits the toxicity of Ag^+ nanomaterials to organisms (Collin et al., 2016) due to decreasing the Ag^+release from the DOM-coated particles.

4. Conclusions

In this study, we demonstrated that the size and chemical composition of NPD influence the sorption of Ag ions onto the NPD under environmentally relevant conditions. We kept the particle number concentration equal for all treatments. Our findings showed that the 600 nm PS-NPD ad/absorb a higher quantity of Ag^+ compared to the 300 nm PS-NPD and PE-NPD when the same particle number concentration was used. However, different dose metrics, such as particle mass and surface area, may result in different outcomes. We used particle number as the dose metric because it was reported to be more suitable for determining the influence of nanomaterial physicochemical properties on their toxicity (Abdolahpur Monikh et al. 2019b). However, the toxicity of Ag^+ in the presence of the 300 nm PS-NPD and PE-NPD was higher than in the presence of the 600 nm PS-NPD. This implies that smaller particles of NPD can be potentially more hazardous than the larger NPD even if they sorb a lower quantity of contaminants. PS-NPD sorbed a higher quantity of Ag^+ ions compared to PE-NPD of the same size. However, the toxicity of Ag^+ in the presence of PE-NPD was higher in few cases. This suggests that chemical composition can influence the toxicity of NPD. This requires further research as most of the current publications focus solely on PS-NPD. The presence of DOM decreased the sorption of Ag^+ onto 600 nm PS-NPD, while it increased the sorption of Ag^+ onto 300 PS-NPD and PE-NPD. Moreover, DOM inhibited the toxicity of Ag-NPD regardless of NPD size. Our findings suggest that the presence of DOM in natural freshwater may inhibit the Trojan horse effects of NPD, however, in some ecosystems, e.g. marine ecosystems, where the concentration of DOM is low, Trojan horse effects of NPD may become a critical issue. We demonstrated that the chemical composition and particle size of NPD are fundamentally important factors to determine the Trojan horse effects in organisms. Further studies may focus on how the other environmental parameters such as salinity and pH influence the sorption and subsequent Trojan horse effects of NPD following our experimental setups.

Declaration of Competing Interest

There are no conflicts to declare.

Acknowledgements

This work was supported by the project PATROLS of European Union's Horizon 2020 research and innovation program under Grant number 760813.

Supplementary materials

Supplementary material associated with this article can be found, in the online version, at doi:10.1016/j.watres.2020.116410.

References

Abdolahpur Monikh, F., Chupani, L., Vijver, M.G., Vancova, M., Peijnenburg, W.J.G.M., 2019a. Analytical approaches for characterizing and quantifying engineered nanoparticles in biological matrices from an (eco)toxicological perspective: old challenges, new methods and techniques. Sci. Total Environ. 660, 1283–1293.

Abdolahpur Monikh, F., Fryer, B., Arenas-Lago, D., Vijver, M.G., Krishna Darbha, G., Valsami-Jones, E., Peijnenburg, W.J.G.M., 2019b. A Dose metrics perspective on the association of gold nanomaterials with algal cells. Environ. Sci. Technol. Lett. 6 (12), 732–738.

Abdolahpur Monikh, F., Grundschober, N., Romeijn, S., Arenas-Lago, D., Vijver, M.G., Jiskoot, W., Peijnenburg, W.J.G.M., 2019c. Development of methods for extraction and analytical characterization of carbon-based nanomaterials (nanoplastics and carbon nanotubes) in biological and environmental matrices by asymmetrical flow field-flow fractionation. Environ. Pollut. 255, 113304.

Al-Sid-Cheikh, M., Rowland, S.J., Stevenson, K., Rouleau, C., Henry, T.B., Thompson, R.C., 2018. Uptake, whole-body distribution, and depuration of nanoplastics by the scallop pecten maximus at environmentally realistic concentrations. Environ. Sci. Technol. 52 (24), 14480–14486.

Alimi, O.S., Farner Budarz, J., Hernandez, L.M., Tufenkji, N., 2018. Microplastics and nanoplastics in aquatic environments: aggregation, deposition, and enhanced contaminant transport. Environ. Sci. Technol. 52 (4), 1704–1724.

Arenas-Lago, D., Abdolahpur Monikh, F., Vijver, M.G., Peijnenburg, W.J.G.M., 2019. Dissolution and aggregation kinetics of zero valent copper nanoparticles in (simulated) natural surface waters: simultaneous effects of pH, NOM and ionic strength. Chemosphere 226, 841–850.

Bakir, A., Rowland, S.J., Thompson, R.C., 2012. Competitive sorption of persistent organic pollutants onto microplastics in the marine environment. Mar. Pollut. Bull. 64 (12), 2782–2789.

Bergmeyer, H.U., 1974. Methods of Enzymatic Analysis. Verlag Chemie; Academic Press, Weinheim; New York.

Bianchini, A., Wood, C.M., 2003. Mechanism of acute silver toxicity in Daphnia magna. Environ. Toxicol. Chem. 22 (6), 1361–1367.

Bury, N.R., Galvez, F., Wood, C.M., 1999a. Effects of chloride, calcium, and dissolved organic carbon on silver toxicity: comparison between rainbow trout and fathead minnows. Environ. Toxicol. Chem. 18 (1), 56–62.

Bury, N.R., McGeer, J.C., Wood, C.M., 1999b. Effects of altering freshwater chemistry on physiological responses of rainbow trout to silver exposure. Environ. Toxicol. Chem. 18 (1), 49–55.

Chae, Y., An, Y.-J., 2017. Effects of micro- and nanoplastics on aquatic ecosystems: current research trends and perspectives. Mar. Pollut. Bull. 124 (2), 624–632.

Chaves, M.L., Costa, J.L., Chainho, P., Costa, M.J., Prat, N., 2011. Are Water Framework Directive stream types biologically relevant? The case of the Mondego river. Portugal. Annales De Limnologie-Int. J. Limnol. 47 (2), 119–131.

Chen, Q., Yin, D., Jia, Y., Schiwy, S., Legradi, J., Yang, S., Hollert, H., 2017. Enhanced uptake of BPA in the presence of nanoplastics can lead to neurotoxic effects in adult zebrafish. Sci. Total Environ. 609, 1312–1321.

Chen, Q., Yin, D., Zhu, S., Hu, X., 2012. Adsorption of cadmium(II) on humic acid coated titanium dioxide. J Colloid Interface Sci. 367 (1), 241–248.

Collin, B., Tsyusko, O.V., Starnes, D.L., Unrine, J.M., 2016. Effect of natural organic matter on dissolution and toxicity of sulfidized silver nanoparticles to Caenorhabditis elegans. Environ. Sci.: Nano 3 (4), 728–736.

Davranche, M., Veclin, C., Pierson-Wickmann, A.-C., El Hadri, H., Grassl, B., Rowenczyk, L., Dia, A., Ter Halle, A., Blancho, F., Reynaud, S., Gigault, J., 2019. Are nanoplastics able to bind significant amount of metals? The lead example. Environ. Pollut. 249, 940–948.

Dong, Z., Qiu, Y., Zhang, W., Yang, Z., Wei, L., 2018. Size-dependent transport and retention of micron-sized plastic spheres in natural sand saturated with seawater. Water Res. 143, 518–526.

Drotar, A., Phelps, P., Fall, R., 1985. Evidence for glutathione peroxidase activities in cultured plant cells. Plant Sci. 42 (1), 35–40.

Enfrin, M., Dumée, L.F., Lee, J., 2019. Nano/microplastics in water and wastewater treatment processes – Origin, impact and potential solutions. Water Res. 161, 621–638.

Fadare, O.O., Wan, B., Guo, L.-.H., Xin, Y., Qin, W., Yang, Y., 2019. Humic acid alleviates the toxicity of polystyrene nanoplastic particles to Daphnia magna. Environ.Sci.: Nano 6 (5), 1466–1477.

Gaspar, T.R., Chi, R.J., Parrow, M.W., Ringwood, A.H., 2018. Cellular bioreactivity of micro- and nano-plastic particles in oysters. Front. Mar. Sci. 5 (345).
Glover, C.N., Playle, R.C., Wood, C.M., 2005. Heterogeneity of natural organic matter amelioration of silver toxicity to Daphnia magna: effect of source and equilibration time. Environ. Toxicol. Chem. 24 (11), 2934–2940.
Gomes, S.I.L., Hansen, D., Scott-Fordsmand, J.J., Amorim, M.J.B., 2015. Effects of silver nanoparticles to soil invertebrates: oxidative stress biomarkers in Eisenia fetida. Environ. Pollut. 199, 49–55.
Hanna, S.K., Montoro Bustos, A.R., Peterson, A.W., Reipa, V., Scanlan, L.D., Hosbas Coskun, S., Cho, T.J., Johnson, M.E., Hackley, V.A., Nelson, B.C., Winchester, M.R., Elliott, J.T., Petersen, E.J., 2018. Agglomeration of escherichia coli with positively charged nanoparticles can lead to artifacts in a standard caenorhabditis elegans toxicity assay. Environ. Sci. Technol. 52 (10), 5968–5978.
He, L., Rong, H., Wu, D., Li, M., Wang, C., Tong, M., 2020. Influence of biofilm on the transport and deposition behaviors of nano- and micro-plastic particles in quartz sand. Water Res. 178, 115808.
Heinlaan, M., Kasemets, K., Aruoja, V., Blinova, I., Bondarenko, O., Lukjanova, A., Khosrovyan, A., Kurvet, I., Pullerits, M., Sihtmäe, M., Vasiliev, G., Vija, H., Kahru, A., 2020. Hazard evaluation of polystyrene nanoplastic with nine bioassays did not show particle-specific acute toxicity. Sci. Total Environ. 707, 136073.
Hogstrand, C., Galvez, F., Wood, C.M., 1996. Toxicity, silver accumulation and metallothionein induction in freshwater rainbow trout during exposure to different silver salts. Environ. Toxicol. Chem. 15 (7), 1102–1108.
Iskrenova-Tchoukova, E., Kalinichev, A.G., Kirkpatrick, R.J., 2010. Metal cation complexation with natural organic matter in aqueous solutions: molecular dynamics simulations and potentials of mean force. Langmuir 26 (20), 15909–15919.
Jeong, C.-.B., Kang, H.-.M., Lee, Y.H., Kim, M.-.S., Lee, J.-.S., Seo, J.S., Wang, M., Lee, J.-.S., 2018. Nanoplastic ingestion enhances toxicity of Persistent Organic Pollutants (POPs) in the monogonont rotifer brachionus koreanus via Multixenobiotic Resistance (MXR) Disruption. Environ. Sci. Technol. 52 (19), 11411–11418.
Jeong, C.-.B., Won, E.-.J., Kang, H.-.M., Lee, M.-.C., Hwang, D.-.S., Hwang, U.-.K., Zhou, B., Souissi, S., Lee, S.-.J., Lee, J.-.S., 2016. Microplastic size-dependent toxicity, oxidative stress induction, and p-JNK and p-p38 activation in the monogonont rotifer (Brachionus koreanus). Environ. Sci. Technol. 50 (16), 8849–8857.
Kalčíková, G., Skalar, T., Marolt, G., Jemec Kokalj, A., 2020. An environmental concentration of aged microplastics with adsorbed silver significantly affects aquatic organisms. Water Res. 175, 115644.
Karlsson, T., Persson, P., Skyllberg, U., 2005. Extended x-ray absorption fine structure spectroscopy evidence for the complexation of cadmium by reduced sulfur groups in natural organic matter. Environ. Sci. Technol. 39 (9), 3048–3055.
Kim, D., Chae, Y., An, Y.-.J., 2017. Mixture toxicity of nickel and microplastics with different functional groups on daphnia magna. Environ. Sci. Technol. 51 (21), 12852–12858.
Kim, H., Kim, J.-.S., Kim, P.-.J., Won, E.-.J., Lee, Y.-.M., 2018. Response of antioxidant enzymes to Cd and Pb exposure in water flea Daphnia magna: differential metal and age — Specific patterns. Comp. Biochem. Physiol. C Toxicol. Pharmacol. 209, 28–36.
Koelmans, A.A., Bakir, A., Burton, G.A., Janssen, C.R., 2016. Microplastic as a vector for chemicals in the aquatic environment: critical review and model-supported reinterpretation of empirical studies. Environ. Sci. Technol. 50 (7), 3315–3326.
Koelmans, A.A., Mohamed Nor, N.H., Hermsen, E., Kooi, M., Mintenig, S.M., De France, J., 2019. Microplastics in freshwaters and drinking water: critical review and assessment of data quality. Water Res. 155, 410–422.
Kungolos, A., Samaras, P., Tsiridis, V., Petala, M., Sakellaropoulos, G., 2006. Bioavailability and toxicity of heavy metals in the presence of natural organic matter. J. Environ. Sci. Health, Part A 41 (8), 1509–1517.
Lee, H., Shim, W.J., Kwon, J.-.H., 2014. Sorption capacity of plastic debris for hydrophobic organic chemicals. Sci. Total Environ. 470-471, 1545–1552.
Lee, W.S., Cho, H.-.J., Kim, E., Huh, Y.H., Kim, H.-.J., Kim, B., Kang, T., Lee, J.-.S., Jeong, J., 2019. Bioaccumulation of polystyrene nanoplastics and their effect on the toxicity of Au ions in zebrafish embryos. Nanoscale 11 (7), 3173–3185.
Liu, J.-f., Zhao, Z.-s., Jiang, G.-b., 2008. Coating Fe3O4 magnetic nanoparticles with humic acid for high efficient removal of heavy metals in water. Environ. Sci. Technol. 42 (18), 6949–6954.
Liu, J., Ma, Y., Zhu, D., Xia, T., Qi, Y., Yao, Y., Guo, X., Ji, R., Chen, W., 2018. Polystyrene nanoplastics-enhanced contaminant transport: role of irreversible adsorption in glassy polymeric domain. Environ. Sci. Technol. 52 (5), 2677–2685.
Liu, Z., Yu, P., Cai, M., Wu, D., Zhang, M., Huang, Y., Zhao, Y., 2019. Polystyrene nanoplastic exposure induces immobilization, reproduction, and stress defense in the freshwater cladoceran Daphnia pulex. Chemosphere 215, 74–81.
Ma, Y., Huang, A., Cao, S., Sun, F., Wang, L., Guo, H., Ji, R., 2016. Effects of nanoplastics and microplastics on toxicity, bioaccumulation, and environmental fate of phenanthrene in fresh water. Environ. Pollut. 219, 166–173.
MARKLUND, S., MARKLUND, G., 1974. Involvement of the superoxide anion radical in the autoxidation of pyrogallol and a convenient assay for superoxide dismutase. Eur. J. Biochem. 47 (3), 469–474.
Materić, D., Kasper-Giebl, A., Kau, D., Anten, M., Greilinger, M., Ludewig, E., van Sebille, E., Röckmann, T., Holzinger, R., 2020. Micro- and nanoplastics in alpine snow: a new method for chemical identification and (Semi) quantification in the nanogram range. Environ. Sci. Technol. 54 (4), 2353–2359.
Murphy, R.J., Lenhart, J.J., Honeyman, B.D., 1999. The sorption of thorium (IV) and uranium (VI) to hematite in the presence of natural organic matter. Colloids Surf. A 157 (1), 47–62.
Naasz, S., Altenburger, R., Kühnel, D., 2018. Environmental mixtures of nanomaterials and chemicals: the Trojan-horse phenomenon and its relevance for ecotoxicity. Sci. Total Environ. 635, 1170–1181.
OECD (2004) Test No. 202: daphnia sp. Acute immobilisation test.
Ogata, Y., Takada, H., Mizukawa, K., Hirai, H., Iwasa, S., Endo, S., Mato, Y., Saha, M., Okuda, K., Nakashima, A., Murakami, M., Zurcher, N., Booyatumanondo, R., Zakaria, M.P., Dung, L.Q., Gordon, M., Miguez, C., Suzuki, S., Moore, C., Karapanagioti, H.K., Weerts, S., McClurg, T., Burres, E., Smith, W., Velkenburg, M.V., Lang, J.S., Lang, R.C., Laursen, D., Danner, B., Stewardson, N., Thompson, R.C., 2009. International pellet watch: global monitoring of persistent organic pollutants (POPs) in coastal waters. 1. Initial phase data on PCBs, DDTs, and HCHs. Mar. Pollut. Bull. 58 (10), 1437–1446.
Oriekhova, O., Stoll, S., 2018. Heteroaggregation of nanoplastic particles in the presence of inorganic colloids and natural organic matter. Environ. Sci.: Nano 5 (3), 792–799.
Pascall, M.A., Zabik, M.E., Zabik, M.J., Hernandez, R.J., 2005. Uptake of Polychlorinated Biphenyls (PCBs) from an aqueous medium by polyethylene, polyvinyl chloride, and polystyrene films. J. Agric. Food Chem. 53 (1), 164–169.
Poynton, H.C., Varshavsky, J.R., Chang, B., Cavigiolio, G., Chan, S., Holman, P.S., Loguinov, A.V., Bauer, D.J., Komachi, K., Theil, E.C., Perkins, E.J., Hughes, O., Vulpe, C.D., 2007. Daphnia magna Ecotoxicogenomics provides mechanistic insights into metal toxicity. Environ. Sci. Technol. 41 (3), 1044–1050.
Qiao, R., Lu, K., Deng, Y., Ren, H., Zhang, Y., 2019. Combined effects of polystyrene microplastics and natural organic matter on the accumulation and toxicity of copper in zebrafish. Sci. Total Environ. 682, 128–137.
Rist, S., Baun, A., Hartmann, N.B., 2017. Ingestion of micro- and nanoplastics in Daphnia magna – quantification of body burdens and assessment of feeding rates and reproduction. Environ. Pollut. 228, 398–407.
Rochman, C.M., Hoh, E., Hentschel, B.T., Kaye, S., 2013a. Long-term field measurement of sorption of organic contaminants to five types of plastic pellets: implications for plastic marine debris. Environ. Sci. Technol. 47 (3), 1646–1654.
Rochman, C.M., Hoh, E., Kurobe, T., Teh, S.J., 2013b. Ingested plastic transfers hazardous chemicals to fish and induces hepatic stress. Sci. Rep. 3 (1), 3263.
Roy, R.L., Campbell, P.G.C., 1997. Decreased toxicity of Al to Juvenile Atlantic salmon (Salmo salar) in acidic soft water containing natural organic matter: a test of the free-ion model. Environ. Toxicol. Chem. 16 (9), 1962–1969.
Shams, M., Alam, I., Chowdhury, I., 2020. Aggregation and stability of nanoscale plastics in aquatic environment. Water Res. 171, 115401.
Shen, M.-.H., Zhou, X.-.X., Yang, X.-.Y., Chao, J.-.B., Liu, R., Liu, J.-.F., 2015. Exposure Medium: key in identifying free Ag+ as the exclusive species of silver nanoparticles with acute toxicity to Daphnia magna. Sci Rep. 5 (1), 9674.
Sobhani, Z., Zhang, X., Gibson, C., Naidu, R., Megharaj, M., Fang, C., 2020. Identification and visualisation of microplastics/nanoplastics by Raman imaging (i): down to 100nm. Water Res. 174, 115658.
Sun, X., Chen, B., Li, Q., Liu, N., Xia, B., Zhu, L., Qu, K., 2018. Toxicities of polystyrene nano- and microplastics toward marine bacterium Halomonas alkaliphila. Sci. Total Environ. 642, 1378–1385.
Tian, X., Li, T., Yang, K., Xu, Y., Lu, H., Lin, D., 2012. Effect of humic acids on physicochemical property and Cd(II) sorption of multiwalled carbon nanotubes. Chemosphere 89 (11), 1316–1322.
Tourinho, P.S., Kočí, V., Loureiro, S., van Gestel, C.A.M., 2019. Partitioning of chemical contaminants to microplastics: sorption mechanisms, environmental distribution and effects on toxicity and bioaccumulation. Environ. Pollut. 252, 1246–1256.
Toussaint, B., Raffael, B., Angers-Loustau, A., Gilliland, D., Kestens, V., Petrillo, M., Rio-Echevarria, I.M., Van den Eede, G., 2019. Review of micro- and nanoplastic contamination in the food chain. Food Additives & Contaminants: Part A 36 (5), 639–673.
Vale, G., Franco, C., Diniz, M.S., Santos, M.M.C.d, Domingos, R.F., 2014. Bioavailability of cadmium and biochemical responses on the freshwater bivalve Corbicula fluminea – the role of TiO2 nanoparticles. Ecotoxicol. Environ. Saf. 109, 161–168.
Velzeboer, I., Kwadijk, C.J.A.F., Koelmans, A.A., 2014. Strong Sorption of PCBs to nanoplastics, microplastics, carbon nanotubes, and fullerenes. Environ. Sci. Technol. 48 (9), 4869–4876.
Wang, W., Wang, J., 2018. Comparative evaluation of sorption kinetics and isotherms of pyrene onto microplastics. Chemosphere 193, 567–573.
Wang, Z., Zhang, L., Zhao, J., Xing, B., 2016. Environmental processes and toxicity of metallic nanoparticles in aquatic systems as affected by natural organic matter. Environ. Sci.: Nano 3 (2), 240–255.
Wu, C., Zhang, K., Huang, X., Liu, J., 2016. Sorption of pharmaceuticals and personal care products to polyethylene debris. Environ. Sci. Pollut. Res. 23 (9), 8819–8826.
Xia, X., Chen, X., Zhao, X., Chen, H., Shen, M., 2012. Effects of carbon nanotubes, chars, and ash on bioaccumulation of perfluorochemicals by chironomus plumosus larvae in sediment. Environ. Sci. Technol. 46 (22), 12467–12475.
Yu, F., Yang, C., Zhu, Z., Bai, X., Ma, J., 2019. Adsorption behavior of organic pollutants and metals on micro/nanoplastics in the aquatic environment. Sci. Total Environ. 694, 133643.
Zhan, Z., Wang, J., Peng, J., Xie, Q., Huang, Y., Gao, Y., 2016. Sorption of 3,3′,4,4′-tetrachlorobiphenyl by microplastics: a case study of polypropylene. Mar. Pollut. Bull. 110 (1), 559–563.
Zhu, K., Jia, H., Sun, Y., Dai, Y., Zhang, C., Guo, X., Wang, T., Zhu, L., 2020. Long-term phototransformation of microplastics under simulated sunlight irradiation in aquatic environments: roles of reactive oxygen species. Water Res. 173, 115564.
Ziccardi, L.M., Edgington, A., Hentz, K., Kulacki, K.J., Kane Driscoll, S., 2016. Microplastics as vectors for bioaccumulation of hydrophobic organic chemicals in the marine environment: a state-of-the-science review. Environ. Toxicol. Chem. 35 (7), 1667–1676.